

# Heat Transfer Behavior of $Al_2O_3$ -Water Nanofluid in Confined Cavity Heated From the Bottom

Houda Jalali<sup>1</sup>, Hassen Abbassi<sup>2</sup>

<sup>1,2</sup>Unit of Computational Fluid Dynamics and Transfer Phenomena, Department of mechanical engineering, National Engineering School of Sfax, University of Sfax, Tunisia

**Abstract:** *This article presents a numerical study of heat transfer in a square cavity filled with water- $Al_2O_3$  nanofluid and heated from the bottom. Mass Conservation, momentum, and energy equations are solved numerically by the finite volume method using the SIMPLER algorithm for pressure-velocity coupling. The effects of the thermal conductivity, the dynamic viscosity, the Rayleigh number, the solid volume fraction and the particle size on heat transfer by  $Al_2O_3$ -water nanofluid were discussed. In this paper, two correlations for viscosity and thermal conductivity of  $Al_2O_3$ -water nanofluid as functions of nanosolid concentration and diameter size are proposed. The numerical results have shown that the heat transfer is influenced by the particle size, the solid volume fraction and Rayleigh number. Results have clearly revealed the appearance of a hysteresis behavior of flow structure and heat transfer when increasing and decreasing the Rayleigh number.*

**Keywords:**  $Al_2O_3$ -water, heat transfer, hysteresis behavior, nanofluids

## 1. Introduction

Nanofluid is a mixture of base fluid and solid particles of sizes less than  $\sim 100$ nm. This type of fluid was firstly studied by Choi [1]. He found that the dispersion of solid nanoparticles into fluid like water, ethylene glycol or oil leads to considerable changement of thermal properties of nanofluid. Since this study, a research axis has been born; nanofluids. The purpose is find fluids with better physical properties which can be used for industrial purposes and meet the requirement of heat transfer increasingly intense. In this context, Eastman et al. [2] studied Cu-ethylene glycol nanofluid. They indicated that the thermal conductivity undergoes an increase in the order of 40% with an addition of 3% solid volume fraction of Cu nanoparticles. The addition of nanosolids into basic liquid leads to an augmentation not only of thermal conductivity, but also of the dynamic viscosity. Wang et al. [3] observed that the effective viscosity of  $Al_2O_3$ -water nanofluid is increased by 86% for 5% volume fraction. Brinkman [4] proposed a theoretical model of dynamic viscosity and clarified that the dynamic viscosity of  $Al_2O_3$ -water nanofluid is  $0.0011 Pa.s$  for 5% nanosolid concentration. For the same concentration, Nguyen et al. [5] reveal, experimentally, that the viscosity is  $0.002 Pa.s$ ; the deviation of 45% of the theoretical model from to the experiment is computed. We noticed that theoretical model of Brinkman [4] underestimate the viscosity of the nanofluid.

The literature includes a considerable amount of numerical and experimental studies that concern the heat transfer by natural convection of nanofluids in a heated enclosure filled by different kinds of nanofluids. Authors [6]-[9] studied heat transfer by natural convection in heated cavity using different types of nanofluids. They observed that addition of nanoparticles into base fluid enhances the heat transfer. Natural convection in enclosures filled with  $Al_2O_3$ -water nanofluid has been investigated by Nasrin et al. [10]. Their results indicate that the heat transfer is most effective when increasing the concentration of solid particle and Prandtl number as well as decreasing aspect ratios. With reference to the above mentioned bibliography, it appears that addition of nanosolids in basic fluid enhances heat

transfer. These studies used theoretical models for viscosity and thermal conductivity such as Brinkman [4], Batchelor [11] and Maxwell [12] models. On the other hand, the recent works, available in the literature, have shown that the dispersion of nanosolids into base fluid leads to a decrease in the heat transfer. These studies used models of viscosity and thermal conductivity nanofluids based on experimental data. Among these, Santra et al. [13] studied heat transfer characteristics of copper-water nanofluid in a differentially heated square cavity with different viscosity models, the Brinkman [4] model and also from experimental model of Kwak and Kim [14]. Results reveal that for the first viscosity model heat transfer increases, but it decreases for the second model. Ho et al. [15] presented a numerical study of natural convection heat transfer of  $Al_2O_3$ -water nanofluid in vertical square enclosures of three different sizes; this study is conducted for high Rayleigh numbers. They observed that at 4% of solid volume fraction, a 20% reduction of the heat transfer coefficient is detected. Putra et al. [16] experimentally investigated natural convection heat transfer of  $Al_2O_3$ -water and CuO-water nanofluids inside a horizontal cylinder heated from one end and cooled from the other. They found deterioration in natural convective heat transfer with increasing particle concentration.

Flow structure inside a cavity heated from the bottom is very unstable; it depends strongly on thermal and dynamic boundary conditions, as well as initial fields as discussed later. In this context, the main aim of the present work is to discuss the effects of the thermal boundary conditions in the flow structure and heat transfer characteristics due to natural convection within a square cavity. Subsequently, with a view to study the effect of the solid volume fraction, the diameter particle, the viscosity and the thermal conductivity of  $Al_2O_3$ -water nanofluid on heat transfer, two correlations of viscosity and thermal conductivity of  $Al_2O_3$ -water nanofluid are proposed. These correlations are based on experimental measurements at ambient temperature.

Volume 7 Issue 3, March 2018

[www.ijsr.net](http://www.ijsr.net)

[Licensed Under Creative Commons Attribution CC BY](https://creativecommons.org/licenses/by/4.0/)

## 2. Statement of the Problem

In this study we consider the flow of  $Al_2O_3$ -water nanofluid inside a square cavity heated from the bottom as indicated in figure 1.

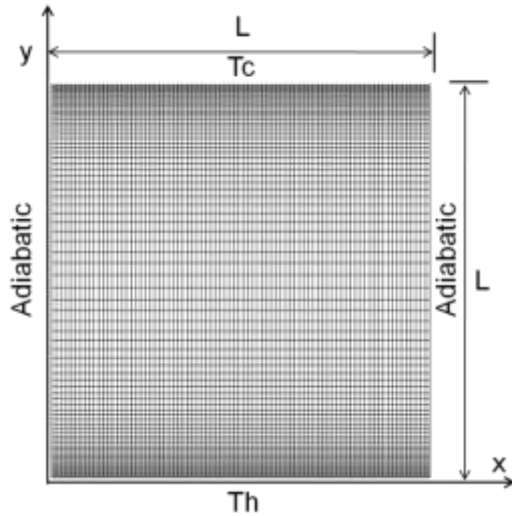


**Figure 1:** Physical configuration

The vertical walls of the cavity are assumed to be insulated while the top and the bottom walls are maintained at a cold temperature  $T_c$  and a hot temperature  $T_h$  respectively. The  $Al_2O_3$ -water nanofluid is considered as Newtonian and incompressible. The flow is supposed to be laminar and bi-dimensional and the Boussinesq approximation is adopted.

## 3. Governing Equation

The two-dimensional numerical solutions of momentum and energy equations were performed to simulate the effects of temperature gradient on the heat transfer in the cavity. Assuming that the solid particles  $Al_2O_3$  are well dispersed in water, therefore we can suppose that physical and thermal properties of the nanofluid are constants as in homogeneous fluid. Thermophysical properties of water and  $Al_2O_3$  nanosolids at room temperature are presented in table 1.

**Table 1:** Physical property of pure water and  $Al_2O_3$  solid particles Oztop et al. [6]

	$k$ ( $W \cdot m^{-1} \cdot K^{-1}$ )	$\rho$ ( $kg \cdot m^{-3}$ )	$C_p$ ( $J \cdot kg^{-1} \cdot K^{-1}$ )	$\beta$ ( $K^{-1}$ )
water	0.613	997.1	4179	$2.1 \cdot 10^{-4}$
$Al_2O_3$	40	3970	765	$8.5 \cdot 10^{-6}$

The density of the nanofluid is expressed as:

$$\rho_{nf} = (1 - \phi)\rho_f + \phi\rho_s \quad (1)$$

The specific heat is given by Oztop et al. [6]:

$$(\rho C_p)_{nf} = [(1 - \phi)(\rho C_p)_f + \phi(\rho C_p)_s] \quad (2)$$

The thermal expansion coefficient is given by Khanafer et al. [7]:

$$(\rho\beta)_{nf} = (1 - \phi)(\rho\beta)_f + \phi(\rho\beta)_s \quad (3)$$

Where  $\phi$  is the solid volume fraction of the nanoparticles and subscripts  $s, f$  and  $nf$  are referred to solid, fluid and nanofluid phases respectively.

Brinkman [4] and Batchelor [11] proposed two models of nanofluid viscosity as a function of solid volume fraction which are expressed, respectively, as:

$$\mu_{nf} = \mu_f(1 - \phi)^{-2.5} \quad (4)$$

$$\mu_{nf} = \mu_f(1 + 2.5\phi + 6.2\phi^2) \quad (5)$$

From experimental measurements of Wang et al. [3], Nguyen et al. [5] and Pak and Cho [17] it appears clearly that the dynamic viscosity of  $Al_2O_3$ -water nanofluid is largely underestimated by theoretical models, especially at high concentrations. This was at the origin of our motivation to find a new and more precise model, taking into consideration the effects of relevant parameters such as concentration and solid particle size. The smoothing of measurements by minimum mean square error method and the Lagrangian polynomial interpolation provide us with the following model for viscosity as a function of concentration  $\phi$  and particle diameter size:

$$\frac{\mu_{nf}}{\mu_f} = \left[ -243.17 \left( \frac{d_f}{d_p} \right)^2 + 11.83 \frac{d_f}{d_p} - 0.0853 \right] \phi^2 + \left[ 1878.4 \left( \frac{d_f}{d_p} \right)^2 - 55.26 \frac{d_f}{d_p} + 0.4027 \right] \phi + 1 \quad (6)$$

$0\% \leq \phi \leq 5\%, 13nm \leq dp \leq 36nm$

Where  $d_p$  and  $d_f$  are the diameters of the spherical nanosolids and  $H_2O$  molecule, respectively.

Figure 2 (a) presents the variation of the relative viscosity of  $Al_2O_3$ -water nanofluid as a function of the solid volume fraction for different diameter size of particles solids. This figure shows clearly that our model given by Eq. (6), predicts acceptably the viscosity. Indeed, the mean deviation of the model to experimental measurement is 3.2%. The relative viscosity significantly increases with increasing concentration and decreases with increasing the diameter of the nanoparticle. The relative viscosity undergoes an increase of 61.53% at  $dp=33nm$  when the solid volume fraction varied from 0 to 3%. At  $dp=28nm$  and  $dp=36nm$ , the variation of the relative viscosity undergoes 44.44% and 31.03% respectively when we pass from 0% to 5% of concentration. More substantially, this figure reveals that the theoretical models of Brinkman [4] and Batchelor [11] models (curves are confounded in figure 2 (a)) underestimate the viscosity, especially at high concentrations and low diameter sizes.

For the thermal nanofluid conductivity, we used experimental measurements of Masuda et al. [18], Eastman et al. [19] and Das et al. [20], therefore, we perform the following model by the same manner as the viscosity:

$$\frac{k_{nf}}{k_f} = \left[ -0.0266 \left( \frac{d_p}{d_f} \right)^2 + 3.8909 \left( \frac{d_p}{d_f} \right) - 148.5075 \right] \phi^2 + \left[ -0.0022 \left( \frac{d_p}{d_f} \right)^2 + 0.2062 \left( \frac{d_p}{d_f} \right) + 4.8860 \right] \phi + 1 \quad (7)$$

$0\% \leq \phi \leq 5\%, 13nm \leq dp \leq 38.4nm$

As illustrated in figure 2 (b) our proposed model of Eq. (7) follows correctly the thermal conductivity behavior of the nanofluid. The deviation of the model with respect to the experimental results is less than 2.3%. This figure shows that the relative thermal conductivity increases with increasing the solid volume fraction and decreases with increasing the

diameter size. At  $dp=13\text{nm}$ , the relative thermal conductivity leads to augmentation of 25.92% when to concentration passes from 0% to 5%.

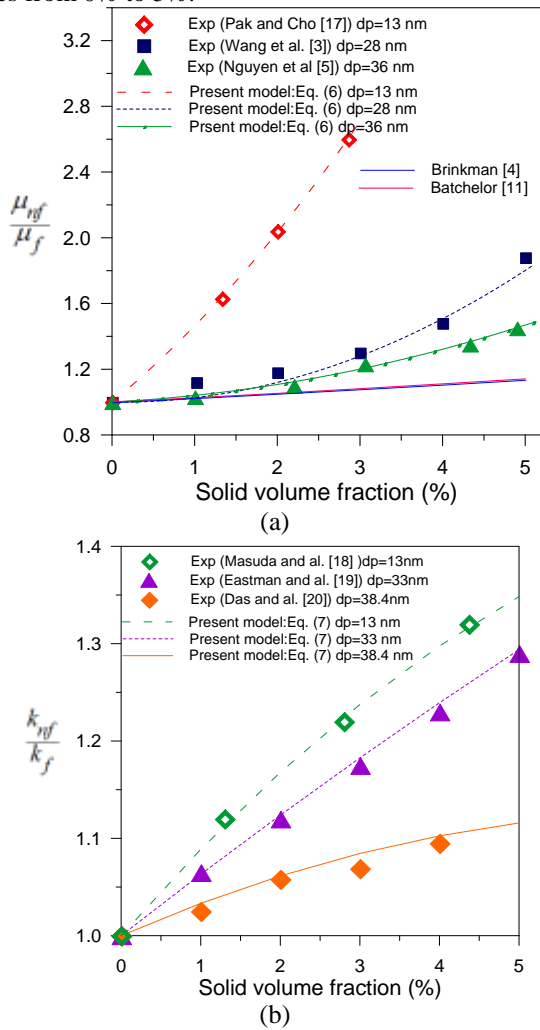


**Figure 2:** Comparison of two proposed models to experiments data, (a)  $\text{Al}_2\text{O}_3$ -water viscosity and (b)  $\text{Al}_2\text{O}_3$ -water thermal conductivity

The mathematical equations describing the nanofluid flow are the continuity, Navier-Stokes and energy equations.

$$\frac{\partial U}{\partial X} + \frac{\partial V}{\partial Y} = 0 \quad (8)$$

$$\frac{\partial U}{\partial \tau} + U \frac{\partial U}{\partial X} + V \frac{\partial U}{\partial Y} = -\frac{\partial P}{\partial X} + \frac{\mu_{nf}}{\rho_{nf} \alpha_f} \left( \frac{\partial^2 U}{\partial X^2} + \frac{\partial^2 U}{\partial Y^2} \right) \quad (9)$$

$$\frac{\partial V}{\partial \tau} + U \frac{\partial V}{\partial X} + V \frac{\partial V}{\partial Y} = -\frac{\partial P}{\partial Y} + \frac{\mu_{nf}}{\rho_{nf} \alpha_f} \left( \frac{\partial^2 V}{\partial X^2} + \frac{\partial^2 V}{\partial Y^2} \right) + \frac{(\rho\beta)_{nf}}{\rho_{nf} \alpha_f} RaPr\theta \quad (10)$$

$$\frac{\partial \theta}{\partial \tau} + U \frac{\partial \theta}{\partial X} + V \frac{\partial \theta}{\partial Y} = \frac{\alpha_{nf}}{\alpha_f} \left( \frac{\partial^2 \theta}{\partial X^2} + \frac{\partial^2 \theta}{\partial Y^2} \right) \quad (11)$$

These equations are normalized by the characteristic height  $L$  of the cavity and the specific velocity  $\frac{\alpha_f}{L}$ , where  $\alpha_f$  is the thermal diffusivity of the basic fluid. The dimensionless temperature is defined as  $\theta = (T - T_c)/(T_h - T_c)$ . The dimensionless numbers that appear in governing equations are the classic Prandtl  $Pr$  and Rayleigh numbers. The dimensionless boundary conditions considered in this study are:

At the verticals walls:  $U = V = 0, \frac{\partial \theta}{\partial X} = 0$

At the top wall:  $U = V = \theta = 0$

At the bottom wall:  $U = V = 0, \theta = 1$

Heat transfer exchanged between the flow and the hot wall is evaluated by the space average Nusselt number expressed for the configuration of figure 1 as:

$$Nu = -\frac{k_{nf}}{k_f} \int_0^1 \frac{\partial \theta}{\partial Y} \Big|_{Y=0} dX \quad (12)$$

When the flow is periodic,  $Nu$  is also averaged over one time period in steady state.

#### 4. Numerical methodology, grid refinement and test validation

The system of equation (8)-(11) is solved using the finite volume method. The SIMPLER algorithm was applied to resolve the pressure velocity coupling in conjunction with an Alternating Direction Implicit (ADI) schema for performing the time evolution. To study the grid independence, we calculate the average Nusselt number at the hot wall for five non uniform grids. The results are related to pure water at  $Ra = 10^5$  and  $Pr$  6.83. Table 2 presents the Nusselt number for different grids. Results show that when we pass from the grid  $71 \times 71$  to the grid  $81 \times 81$ ,  $Nu$  undergoes a variation of 0.25%. When we pass from  $81 \times 81$  to the grid  $91 \times 91$ , the variation of  $Nu$  is only 0.024%. We conclude that the grid of  $81 \times 81$  gives a good compromise between precision and calculation time and it is sufficient to carry out a numerical study of this flow.

**Table 2:** Variation of Nusselt number versus grid mesh

Grid	51x51	61x61	71x71	81x81	91x91
Nusselt	4.1203	4.1156	4.1025	4.0921	4.0911

For validation purpose, we present in Table 3 a comparison between our results and those of Ghasemi and Aminossadati [8]. The maximum difference between results concerning the Nusselt number  $Nu$  is less than 1.76%. We conclude that our simulations give acceptable results.

**Table 3:** Validation tests

Ra	$10^3$	$10^4$	$10^5$
Nu (Present study)	1.0010	2.1972	4.0921
Nu (Ghasemi and Aminossadati [8])	1.0030	2.1950	4.0201

### 5. Results and Discussion

The influence of thermal conductivity and dynamic viscosity via the two new correlation developed in this work is presented in this paper. The results have been obtained for a Rayleigh numbers varying from  $10^3$  to  $10^5$ . The solid volume fraction is varied from 0% to 5%, with the nanoparticle diameter ranging from 13 nm to 30 nm.

#### 5.1 Effect of initial fields on structure flow and heat transfer

Numerically and even experimentally, when the cavity is heated from bottom, at weak Rayleigh numbers, four structures of the flow are possible; a single vortex appears occupying the entire cavity turning in the clockwise or anticlockwise sense; or two vortices turning in opposite sense ascending or descending in the middle region of the cavity. We estimate that experimentally, one or other of the structures is possible; it depends on some fine details such as the uniformity of the heating or the state of the wall surface. Numerically, we believe that the initial fields of velocity,

temperature and pressure determine the evolution to any structure.

In this section, we start the study by presenting the simulation of the case  $Ra=10^5$  and  $\phi=0\%$ , following two different ways: a) starting from velocity fields equal to zero and temperature field equal to average temperature by directly imposing  $Ra=10^5$ . b) Gradually increasing  $Ra$  until  $Ra=10^5$ . Results are presented in figure 3. Both paths lead to completely different flow structure.

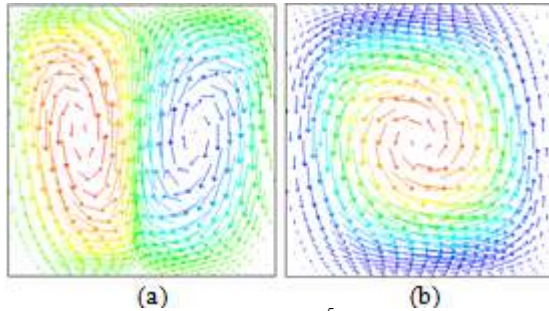


**Figure 3:** Flow structure at  $Ra=10^5$ : (a) Bicellular structure: results are obtained starting from initial velocity field equal to zero (motionless fluid) and temperature field equal to mean temperature. (b) Unicellular structure: gradually increasing  $Ra$  until  $Ra=10^5$

Figure 3 (a) shows that in simulation case a), the flow is characterized by the presence of two symmetric cells turning in the opposite sense inside the cavity, and ascending from the cavity center. The Nusselt number in this case is equal to 4.0921. Figure 3 (b) shows that in the case b) the flow structures in the cavity is of a single vortex and  $Nu=3.8987$ . We deduce that in numerical simulations, the initial fields have a significant effect on the flow structure but they have a small effect on heat transfer, indeed the variation of the

Nusselt number is in order of 4.72%.

In the following simulations, we study the flow structure and heat transfer evolutions by increasing then decreasing the Rayleigh number in order to detect a possible hysteresis behavior. Starting simulations from  $Ra=10^4$  by increasing slowly  $Ra$ . As seen in Figure 4 (A1), we observe the appearance of a single vortex occupying the entire cavity turning in anti-clockwise sense this structure remains the same until  $Ra=2.5 \times 10^5$ . One might ask why it was not the other sense. We estimate that both senses are possible, but the obtained sense is may be ascribed to the random action of small truncation errors and computer's round-off errors [9]. By exceeding  $Ra=2.5 \times 10^5$ , the flow becomes multicellular and periodic. Figure 4 (A2) exhibits the flow structure during one period. It is an alternation between fusions and separations of diametrically opposed cells. At  $Ra=3 \times 10^5$ , the period is found to be 85 seconds. From this situation, as we decrease the Rayleigh number, the flow structure is different to the increasing case; the flow remains multicellular until  $Ra \approx 1.5 \times 10^5$ . For  $Ra=1.5 \times 10^5 - 10^5$ , the flow undergoes a transition and becomes bicellular until  $Ra=10^4$  (see figure 4 A3), cells are turning in opposite sense inside the cavity. The fluid rises from the middle of the hot bottom wall towards the upper cold wall and descends on sides of the enclosure. In the case of nanofluid, at  $\phi=5\%$ , during the increase of the  $Ra$  number and starting from  $Ra=10^4$ , the flow structure into the square cavity becomes multicellular and periodic at  $Ra=1.5 \times 10^6$ . When  $Ra$  decreases, the flow structure undergoes a transition and becomes bicellular at  $Ra = 2.5 \times 10^5$  and  $\phi=5\%$ .

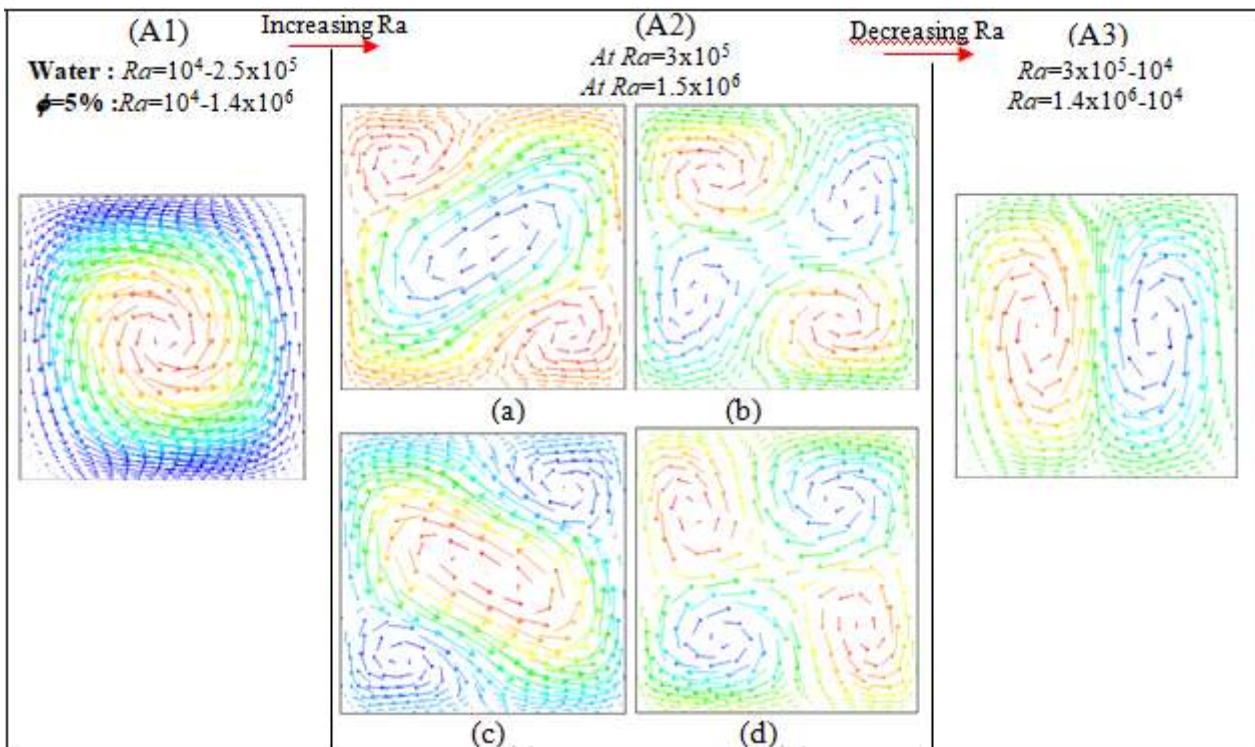
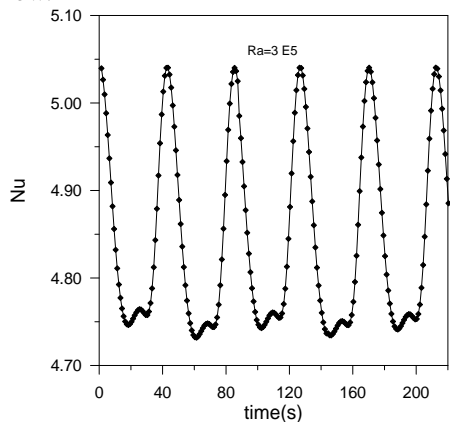
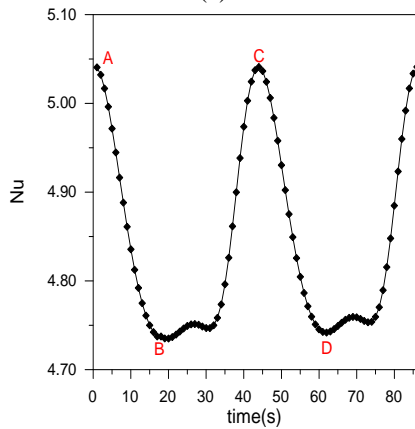


**Figure 4:** Flow structure for increasing and decreasing Rayleigh number

Heat transfer, during the periodic regim of figure 4 (A2), is given in figure 5 and figure 6. The evolution of space average Nusselt number is harmonic but not sinusoidal for  $\phi=0\%$ ; the periodic regim has two maximums and two minimums. Figure 5 (b) and figure 6 (b) present a zoom over one period, at  $\phi=0\%$  and  $\phi=5\%$ , the time periodic is equal to 85s and 60s respectively. The flow structures presented in figure 4 (a), (b), (c) and (d) corresponds to points A, B, C, and D respectively of figure 5 (b) and figure 6 (b). We verified in numerical simulations that maximums of  $Nu$  are recorded when the flow structure is of three cells as in figure 4(a) and figure 4(c), whereas minimums are recorded when the flow structure is of four cells as in figure 4(b) and figure 4(d). We can infer that a flow of three cells is an engine of heat transfer that is more efficient than a flow of four cells during the periodic flow.

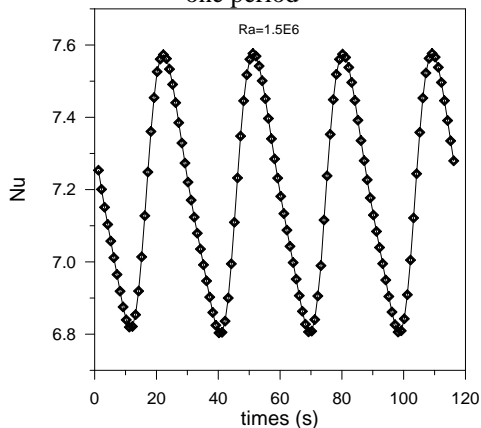


(a)

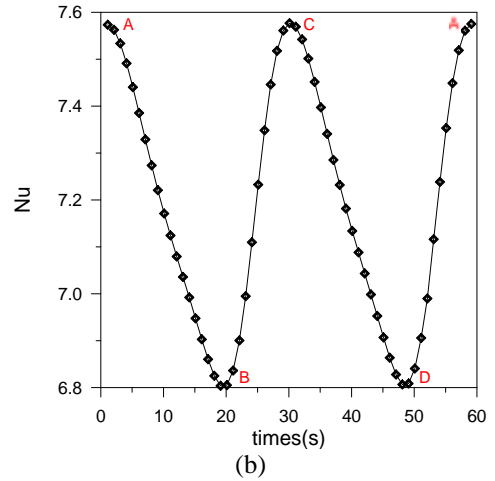


(b)

**Figure 5:** Case of pure water  $\phi=0\%$ : Periodic regim at  $Ra=3 \times 10^5$  (a): Evolution of Nusselt number; (b) Zoom over one period

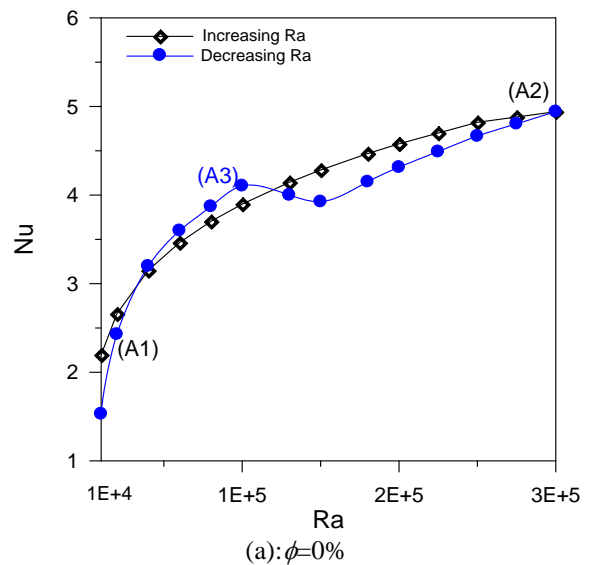


(a)

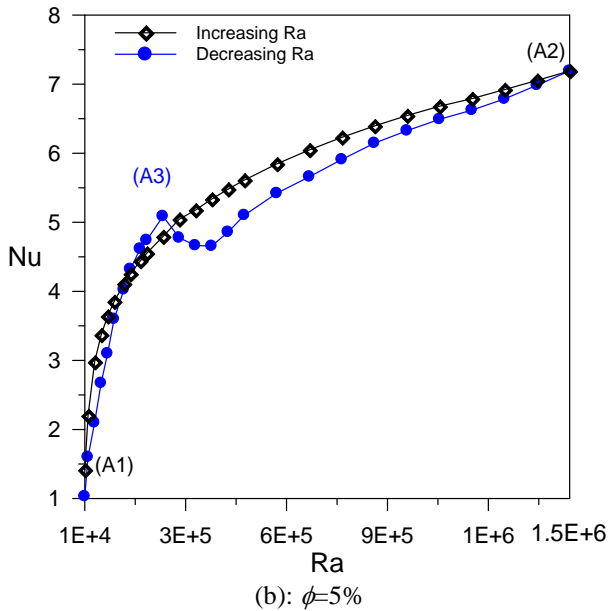


(b)

**Figure 6:** Case of  $\phi=5\%$ : Periodic regim at  $Ra=1.5 \times 10^6$  (a): Evolution of Nusselt number; (b) Zoom over one period  
Figure 7 quantifies the heat transfer from the hot side to the flow in both cases increasing and decreasing  $Ra$ . Curve corresponding to the decrease in  $Ra$  does not follow the same curve as in increasing  $Ra$ ; a hysteresis region is obtained when the  $Ra$  number varies from  $10^4$  up to the value of the appearance of the periodic regim. This hysteresis behavior is in direct relation with the difference in flow structure when increasing and decreasing  $Ra$ . In the case of increasing  $Ra$ , space and time averaged Nusselt number  $Nu$  follows a monotonic increase. For the decreasing of  $Ra$ , the corresponding curve does not coincide with the case of increasing  $Ra$ , and we note a sudden augmentation of the Nusselt number observed in the range of  $Ra$  between  $1.5 \times 10^5$  and  $10^5$  for water as indicated in figure 7 (a). In the case of  $\phi=5\%$ , this range appear between  $4.5 \times 10^5$  and  $2.5 \times 10^5$  as seen in figure 7 (b). This jump is in direct relation with the flow mode transition discussed previously. The jump in  $Nu$  observed can be attributed to change in the flow structure from multicellular to bicellular. It seems that at high Rayleigh numbers, heat transfer is efficient with fewer cells; then when the flow passes from three to two cells, heat transfer increases making the jump seen in figure 7.



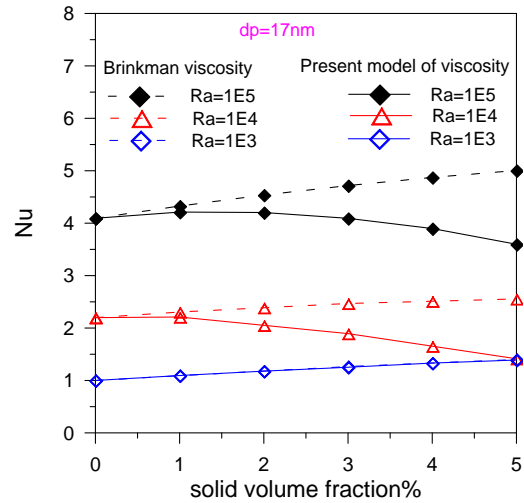
(a):  $\phi=0\%$



**Figure 7:** Nusselt number as a function of Rayleigh number for the cavity heated from bottom for increasing and decreasing  $Ra$ . (a):  $\phi=0\%$  and (b):  $\phi=5\%$  nanofluid  $Al_2O_3$ -water

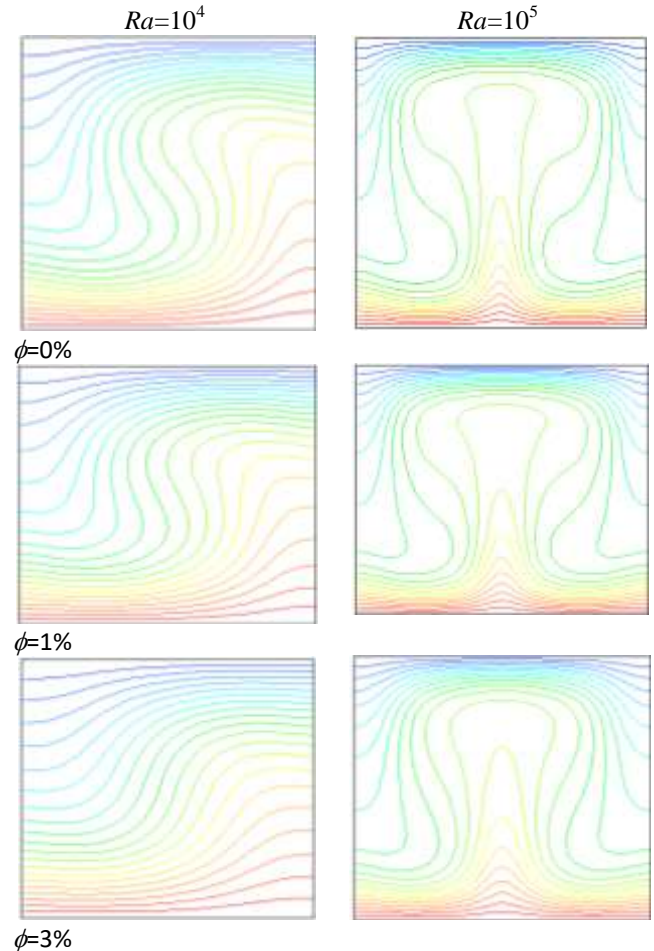
### 5.2 Heat transfer

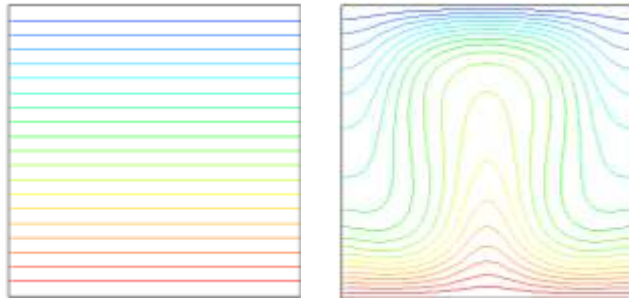
Figure 8 evinces the variation of Nusselt number as a function of solid volume fraction  $\phi$  using our models for dynamic viscosity (eq.6) and thermal conductivity (eq.7) in comparison with results obtained by Brinkman model [4] (eq.4) for viscosity. As seen in figure 8, our models lead to the decrease in Nusselt number when increasing the concentration  $\phi$  except the case  $Ra=10^3$ . This behavior is as pronounced as the Rayleigh number increases. This result seems to be surprising. We presume that, as in most literature, the addition of nanosolids in basic liquid always leads to an increase in heat transfer. The evident question is why our model leads to the decrease in  $Nu$ , whereas Brinkman model leads to an increase. It is noteworthy that the addition of nanosolids plays a double role; it increases the thermal conductivity of the nanofluid and then increases heat transfer, but also increases its viscosity and then slows the flow motion resulting in a decrease in heat transfer. The problem now is which plays the most important role: the increase in viscosity or in thermal conductivity after the addition of nanosolids. By analyzing different models, we remark that at a 5% nanosolids concentration, the thermal conductivity of the nanofluid undergoes an augmentation of a maximum 41.36 %, whereas the augmentation in viscosity is about 206.7 % for our model and 12 % only for Brinkman model. Since our model for viscosity is based on recent experimental results, we think that it is more credible than Brinkman model, which is based on theoretical considerations. Now the behavior of  $Nu$  as a function of  $\phi$  presented in figure 8 is understandable; the increase in nanofluid viscosity after the addition of nanosolids prevails over the increase in thermal conductivity. As a consequence, heat transfer is seen in decrease when increasing the concentration. An exception for  $Ra=10^3$ , where  $Nu$  increases with increasing  $\phi$ . In this case heat transfer by conduction is predominant and then the viscosity plays a secondary role.



**Figure 8:** Nusselt number as a function of solid volume fraction of  $Al_2O_3$  for different Rayleigh numbers: Continuous curves are obtained by our models; Discontinuous curves correspond to Brinkman model for viscosity.

Figure 9 shows the isotherms at different solid volume fraction for  $Ra=10^4$  and  $Ra=10^5$ . At  $Ra=10^4$ , as the solid volume fraction increase as the isotherms becomes parallel to the working walls indicating the tendency to dominance of conduction heat transfer. Nonetheless, at  $Ra=10^5$ , isotherms are very tight in the hot and cold walls especially for the weak concentration. But as the concentration increases, the space between the isotherms adjacent to hot and cold walls increases which is indicative of a decrease in the heat transfer.





$\phi=5\%$   
**Figure 9:** Isotherms for several solid volume fractions at  $Ra=10^4$  and  $Ra=10^5$

### 5.3 Influence of particle sizes on heat transfer

Figure 10 displays the influence of nanoparticle diameter  $dp$  on the Nusselt number  $Nu$  as a function of solid volume fraction. However, figure 10 (a) shows that, for  $dp=30$  nm, the heat transfer at  $\phi$  less than 4% is superior to that of pure water. At  $dp=20$  nm,  $Nu$  undergoes an increase compared to pure water until  $\phi=2.25\%$ . For  $dp=13, 15$  and  $17$  nm the Nusselt number undergoes a decrease of about 54.47%, 43.43% and 34.10% respectively when the solid volume fraction passes from 0% to 5%. Figure 10 (b) shows that for  $dp=13$  nm and  $dp=15$  nm, Nusselt number undergoes a decrease of about 28.25% and 19.15%, respectively, when the solid volume fraction varied from 0% to 5%. This behavior is explained by the augmentation of the viscosity compared to the augmentation of thermal conductivity in this interval of diameter size. Furthermore, for  $dp=17$  nm,  $Nu$  undergoes a slight increase for  $\phi$  less than 3% compared to pure water. On the other hand, for  $dp=20$  nm,  $Nu$  increases remarkably with increasing the solid volume fraction, reaches a maximum near to  $\phi=2\%$ , then decreases slowly but remains superior to the case of pure water up to  $\phi=4.47\%$ . Moreover, when  $dp=30$  nm, the addition of  $Al_2O_3$  nanosolid leads to an increase in heat transfer and reaches a maximum near to 4%. This maximum indicates an augmentation of heat transfer of about 8.99% compared to pure water. From this study, we concluded that the heat transfer by  $Al_2O_3$ -water nanofluid is very influenced by the diameter size of solid particles and by the solid volume fraction.

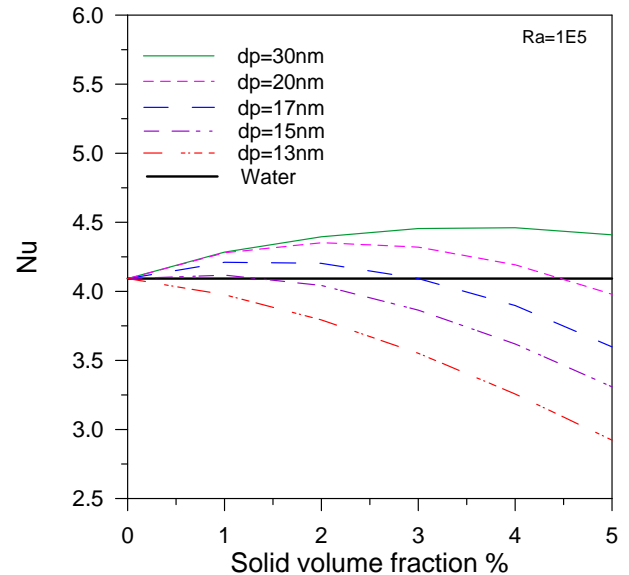
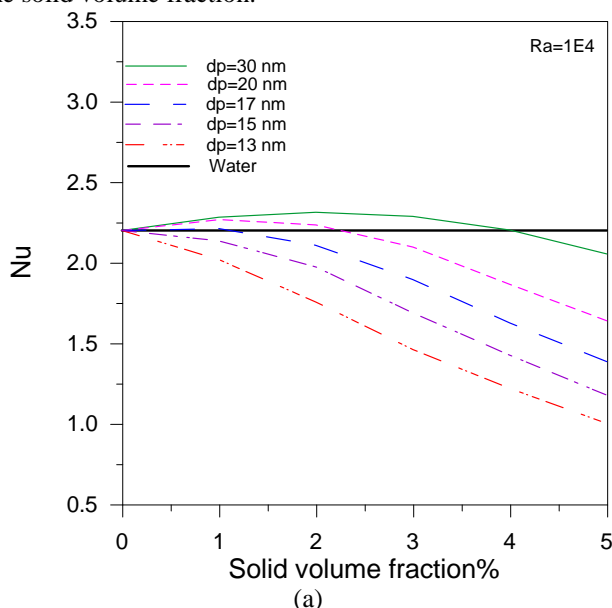


**Figure 10:** Variation of Nusselt number as a function of the solid volume fraction for various nanoparticles size, (a):  $Ra=10^4$  and (b):  $Ra=10^5$ .

### 6. Conclusion

A numerical simulation is performed to study the effect of adding  $Al_2O_3$  nanoparticles in water on the heat transfer in the cavity heated from the bottom. Two correlations for dynamic viscosity and thermal conductivity of  $Al_2O_3$ -water nanofluid, based on experimental results, have been established and discussed. The comparison between the new correlation of dynamic viscosity and Brinkman model, shows that theoretical viscosity model is unable to predict the nanofluid viscosity. It appears that addition of nanosolids into basic liquid leads to a strong increase in viscosity and slight increase in thermal conductivity. As a consequence, augmentation of heat transfer is not guaranteed. The opposite effects of viscosity and thermal conductivity are studied in this paper. It appears that augmentation of heat transfer by the addition of  $Al_2O_3$  is guaranteed only for a range of particles size in a range of solid volume fraction. In general, for low concentrations, the augmentation of heat transfer is obtained only when the particle size exceeds 20 nm.

### References

- [1] S.U.S. Choi, "Enhancing thermal conductivity of fluids with nanoparticles," ASME Fluids Eng. Div, vol. 231, pp. 99-105, 1995.
- [2] J.A. Eastman, S.U.S. Choi, S. Li, W. Yu, and L.J. Thompson, "Anomalous increased effective thermal conductivities of ethylene glycol-based nanofluids containing copper nanoparticles, Applied Physics Letters, vol. 78, pp.718-720, February 2001.
- [3] X. Wang, X. Xu, and S.U.S. Choi, "Thermal conductivity of nanoparticle-fluid mixture," J. Thermophys Heat. Transf., vol. 13, pp. 474-480, October 1999.
- [4] H.C. Brinkman, "The viscosity of concentrated suspensions and solution," J. Chem. Phys., vol. 20, pp. 571-581, December 1952.

- [5] C. Nguyen, F. Desgranges, G. Roy, N. Galanis, T. Mare, S. Boucher, and H. Angue Mintsa, "Temperature and particle-size dependent viscosity data for water-based nanofluids – hysteresis phenomenon," *Int. J. Heat. Fluid. Fl.*, vol. 28, pp. 1492–1506, December 2007.
- [6] H.F. Oztop, E. Abu-Nada, "Numerical study of natural convection in partially heated rectangular enclosures filled with nanofluids," *Int. J. Heat. Fluid. Fl.*, vol. 29, pp. 1326–1336, October 2008.
- [7] K. Khanafer, K. Vafai, and M. Light stone, "Buoyancy-driven heat transfer enhancement in a two-dimensional enclosure utilizing nanofluids," *Int. J. Heat. Mass. Tran.*, vol. 46, pp. 3639-3653, September 2003.
- [8] B. Ghasemi and S.M. Aminossadati, "Natural Convection Heat Transfer in an Inclined Enclosure Filled with a Water-CuO Nanofluid," *Numer. Heat. Tr. A-Apl.*, vol. 55, pp. 807–823, February 2009.
- [9] M. Bouhaleb and H. Abbassi, "Numerical investigation of heat transfer by CuO-water nanofluid in rectangular enclosures," *Heat. Transfer. Eng.*, 37, pp. 13-23, March 2015.
- [10] R. Nasrin, M.A. Alim, and A.J. Chamkha, "Buoyancy-driven heat transfer of water–Al<sub>2</sub>O<sub>3</sub> nanofluid in a closed chamber: Effects of solid volume fraction, Prandtl number and aspect ratio," *Int. J. Heat. Mass. Tran.*, vol. 55, pp. 7355–7365, December 2012
- [11] G. Batchelor, "The effect of Brownian motion on the bulk stress in a suspension of spherical particles," *J. Fluid. Mech.*, vol. 83, pp. 97–117, November 1977.
- [12] J. Maxwell, "A treatise on electricity and magnetism," Clarendon Press, Oxford (U.K.) 1873.
- [13] A.K. Santra, S. Sen and N. Chakraborty, "Study of heat transfer characteristics of copper–water nanofluid in a differentially heated square cavity with different viscosity models," *J. Enhanc. Heat Transf.*, vol.15, pp. 273–287, 2008.
- [14] K. Kwak and C. Kim, "Viscosity and thermal conductivity of copper oxide nanofluid dispersed in ethylene glycol", *Korea-Australia Rheology Journal*, Vol. 17, pp. 35-40, June 2005
- [15] C.J. Ho, W.K. Liu, Y.S. Chang and C.C. Lin, "Natural convection heat transfer of alumina-water nanofluid in vertical square enclosure: an experimental study, *Int. J. Thermal Sci.*, vol.49, pp. 1345–1353, August 2010.
- [16] N. Putra, W. Roetzel and S. K. Das, "Natural convection of nanofluids," *Heat Mass Transfer*, 39(8), pp. 775–784, 2003.
- [17] B.C. Pak, and Y.I. Cho, "Hydrodynamic and heat transfer study of dispersed fluids with submicron metallic oxide particles," *Exp. Heat Transfer: A Journal of Thermal Energy Generation, Transport, Storage, and Conversion*, vol.11, pp. 151–170, Janvier 1999.
- [18] H. Masuda, A. Ebata, K. Teramae and N. Hishinuma, "Alteration of thermal conductivity and viscosity of liquid by dispersing ultra-fine particles. Dispersion of Al<sub>2</sub>O<sub>3</sub>, SiO<sub>2</sub> and TiO<sub>2</sub> ultra-fine particles, *Netsu Bussei*, 4, pp. 227–233, June 1993.
- [19] J.A. Eastman, U.S. Choi, S. Li, L.J. Thompson and S. Lee, "Enhanced thermal conductivity through the development of nanofluids," *Materials Research Society*, vol.457, 3–11, 1997.
- [20] S.K. Das, N. Putra, P. Thiesen and W. Roetzel, "Temperature dependence of thermal conductivity enhancement for nanofluids," *J. Heat Transfer*, vol. 125, pp. 567–574, July 2003.

### Author Profile



**Houda JALALI** is a researcher at the unit of Computational Fluid Dynamics and Transfer Phenomena in the department of Mechanics at the National Engineering School of Sfax-Tunisia. She obtained her Masters in 2013. The subject concerns the flow of liquid metal under the effect of magnetic field. She is currently a Ph. D. student under the supervision of Prof. Hassen Abbassi and working on heat transfer enhancement by nanofluids.



**Hassen ABBASSI** is a professor of Physics at University of Sfax, Tunisia. He obtained his Ph. D. of Physics in 2001 from the Sciences Faculty of Tunis and obtained his Habilitation in 2004 from the University of Sfax. Currently, he directs a research group in the fields of fluid flow and heat transfer at the National Engineering School of Sfax. His research interests include heat exchangers, heat transfer by nanofluids, flows around obstacles, porous media, magneto hydrodynamics and computational fluid dynamics. He has published about 38 research papers in international journals and conferences and a textbook at the Tunisian national center of publication.